

# Kinetic Justification of the Solubility Product: Application of a General Kinetic Dissolution Model

Antonio C. Lasaga<sup>†</sup> and Andreas Lüttge<sup>\*,‡</sup>

*GeoKinetics, P.O. Box 1042, Lemont, Pennsylvania 16851, Department of Earth Science, MS-126, Rice University, P.O. Box 1892, Houston, Texas 77251-1892, and Center for Biological and Environmental Nanotechnology, Rice University, Houston, Texas 77005*

*Received: June 1, 2004; In Final Form: September 20, 2004*

Using a simple, feldspar-like model and the crystal-based reaction mechanism for water–rock kinetics being developed before, we show directly how the dissolution of euhedral faces of crystals are governed by the nonlinear quantity represented by the solubility product. The kinetic approach requires recognition of the essential role played by the correlation of the dynamics of neighboring sites in a crystal, the statistical dynamics of steps, the coupling of the various kink sites on the surface by the crystal structure, and the inclusion of bond formation as well as bond rupture into the kinetic reaction mechanism. The same kinetic approach, which accounts for the role of the solubility product (or  $\Delta G$ ) in the overall rate, is then shown also to explain the observed inhibition behavior in feldspars as well as the often-written phenomenological rate law, involving a product of a pH term, an activation energy term, and a  $\Delta G$  term.

## Introduction

The field of water–mineral kinetics and the dissolution of minerals has been of great interest in the past decades because of its importance to many natural phenomena in the earth's crust, in addition to its central role in understanding man-made and environmental problems. As a result, a large number of chemical studies have been carried out involving many different minerals and aqueous conditions. While these studies have focused on the effect of pH, organic ligands, ionic strength, and temperature on the dissolution rate and have also investigated the changes in surface structure, the formation of alteration products, and the initial nonstoichiometry of the dissolution process, the work has still left a major portion of the overall rate law missing, that is, the dependence of the rate of reaction on the saturation state of the solution. Any hope of understanding the behavior of the solid crust in the presence of water requires that the possibility of achieving equilibrium be included in the kinetic model. Ironically, understanding this variation is, in fact, essential to also properly understanding the pH, temperature, ionic strength effects, or inhibitory effects previously studied.

In the field of crystal growth, the dependence of the rate on the saturation state is one of the most central issues. In part, this concern arises because, in crystal growth, the system is never under conditions where the growth rate is independent of the saturation state. The existence of a region far from equilibrium where the dissolution rate varies very little with saturation state (so-called dissolution plateau) resulted in little work on the saturation-state dependence. At the same time, the lack of data on the saturation-state dependence of mineral dissolution did little to help develop a conceptual link between the statistical process of dissolution, which involves the chemical interactions of many atoms, and the elementary reactions identified in surface speciation schemes (e.g., formation of  $\text{SiOH}_2^+$  or  $\text{SiO}^-$  or  $\text{Al-O-COR}$  surface groups, etc.).

Two well-known models of crystal growth, the dislocation-based Burton, Cabrera, and Frank (BCF) model and the 2D-nucleation model, predict rates that vary strongly with the free energy change of the dissolution reaction,  $\Delta G$ . The screw-dislocation-based mechanism of crystal growth, the BCF mechanism, drives the crystal growth by the self-generating steps of spirals emanating from screw dislocations. This kinetic mechanism leads to the well-known result, eq 1<sup>1,2</sup>

$$\text{Rate} = k\Delta G^2 \tanh(C/\Delta G) \quad (1)$$

In fact, this rate law approaches quadratic behavior for small  $\Delta G$  values (i.e., near equilibrium conditions), eq 2

$$\text{Rate} = A\Delta G^2 \quad (2)$$

and it morphs into a linear law far from equilibrium. This BCF rate law has been verified in numerous growth experiments.<sup>3</sup> While important additional factors enter when dislocations dominate the mode of dissolution,<sup>4,5</sup> certainly, the same spiral mechanism would lead to quadratic rate laws near equilibrium for dissolution.

The second kinetic mechanism, the 2D-nucleation mechanism, is also well-known and established and leads to highly nonlinear rate laws.<sup>2,6</sup> From a calculation of the free energy of formation of a critical 2D nucleus (pancake) or a critical 2D hole (growth and dissolution, respectively), the growth or dissolution rate of a nearly perfect crystal surface (no defects) would obey a rate law given by eq 3

$$\text{Rate} = A e^{-B/|\Delta G|} \quad (3)$$

which decreases enormously as equilibrium conditions are approached.

Interestingly, most reactive flow models in use for ground-water flow modeling, hydrothermal systems, pollution studies, soil formation, and so on, all of which need the dependence of the dissolution rate of materials as a function of the departure

\* To whom correspondence should be addressed. E-mail: aluttge@rice.edu.

<sup>†</sup> GeoKinetics.

<sup>‡</sup> Rice University.

from equilibrium, have simply assumed, in general, a dependence of the rate on  $\Delta G$  given by eq 4

$$\text{Rate} = A(1 - e^{\alpha\Delta G/RT}) \quad (4)$$

where  $\alpha$  is some supposedly “stoichiometric” coefficient related to the elementary reaction controlling the rate (which further assumes that just one reaction does play such a role).<sup>7</sup> But, unlike BCF or nucleation mechanisms, eq 4 is not derived from a detailed model of the crystal dissolution process. Instead, a rate-determining surface molecular complex is postulated, and the rate of the overall dissolution reaction is made proportional to the concentration of this one surface complex. Equation 4 then is arrived at by also making the same complex control the crystal growth and treating the reaction as an elementary reaction or a chain of elementary reactions.<sup>8,9</sup> The commonly used rate law (eq 4) becomes linearly dependent on  $\Delta G$  near equilibrium. In crystal growth studies, the equivalent law to eq 4 is usually termed the Wilson–Frenkel (W–F) growth law;<sup>1</sup> however, the W–F law is given as a limiting law that is usually in stark disagreement with experimental observations from crystal growth experiments.<sup>3,6,10–13</sup> In dissolution kinetic processes, the solubility product is frequently employed to model a rate law such as that in eq 4.<sup>7</sup> However, the justification for how the solubility product emerges from the dynamics of a kinetic mechanism in which the emphasis is on different ions species, which arrive or depart from a surface individually, has not been addressed in the dissolution kinetic literature.<sup>8</sup> The only “justification” for the use of eq 4 is based on results from elementary reactions<sup>14,15</sup> or a chain of elementary reactions under stringent conditions,<sup>9</sup> neither of which are appropriate for the 3D reaction mechanism involved in crystal dissolution.<sup>16,17</sup> The mineral–fluid models, furthermore, focus on the departure of a single Si- or Al-containing surface complex on which to base the kinetic mechanism. Not only does the departure of Si and Al species represent a host of parallel reactions, but more significantly, the departures and arrivals of Si and Al units are all intimately interdependent when a crystal structure is involved.

A thermodynamic treatment of dissolved Al, Si, Fe, and so on, in solution begins with the assumption that the ions are largely independent entities. The image is based on individual hydrated ions or complexes moving pseudorandomly in the aqueous medium. As a consequence, their collisions and interactions with the surface will, in and of themselves, be individualistic and separate events. And yet, when crystal growth or dissolution processes take place, these collisions must be linked; otherwise, the use of  $\Delta G$  in a kinetic model involving individual reactions would not be justified.

In nonequilibrium mineral–fluid situations ( $\Delta G \neq 0$ ), one can still, of course, calculate  $\Delta G$ , using the solubility product. The theory of irreversible thermodynamics postulates that the rate of dissolution or growth will be a linear function of  $\Delta G$ , but this theory is not a mechanistic kinetic theory. Furthermore, it is well-known that this theory is not fully adequate for chemical reactions.<sup>18</sup> Nonetheless, equilibrium requires that there must be a dependence of the rate on  $\Delta G$ , albeit a complex nonlinear one (e.g., eqs 1 and 3). If we are to proceed beyond a mere phenomenological postulate for a  $\Delta G$  dependence as has been done with eq 4, then an understanding of how  $\Delta G$  or the solubility product emerges as the important rate-determining quantity near equilibrium during dissolution or growth needs to be extracted from an adequate kinetic reaction mechanism. Only within such a comprehensive reaction mechanism can

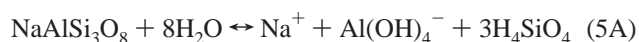
many of the deeper questions of water–rock kinetics be answered satisfactorily.

Given the wide range of defects and mineral structures involved in many natural phenomena in the earth’s crust, a basic question is whether eq 4 can be derived for these situations under any kind of conditions. For monatomic crystals with rough surfaces, one can indeed deduce eq 4 on the basis of simple arguments.<sup>12</sup> However, the much more interesting question of the emergence of  $\Delta G$  in a multicomponent complex mineral structure has not been addressed from a kinetic surface-chemistry point of view. While additional complexities are expected in the dissolution of minerals,<sup>4,5,19,20</sup> it is still quite important to analyze the possible kinetic conditions and surface models, which will validate eq 4 without vague allusions to elementary reactions and using the characteristics of the crystal structures involved. With this analysis, we can then understand the reasons for significant deviations from eq 4 in actual experimental and field conditions.

At the simplest level, the link between individual atom dynamics and the solubility product is provided by the number of available sites at the crystal surface. Thus, for an aluminosilicate, if the aqueous Si concentration increases and the Al concentration decreases, the surface will have an increase in Si-occupied sites and a decrease in Al-occupied sites. However, this change in the surface composition will also diminish the number of available sites for Si attachment and increase the number of sites available for Al attachment. It is this response of the surface to changes in solution composition that is offsetting the concentration imbalance. In addition, the departure rate of Si from the surface would be higher than that of Al, also further offsetting the imbalance. Therefore, as the solubility product implies, one can maintain the same level of equilibrium or disequilibrium by raising  $C_{\text{Si}}$  and lowering  $C_{\text{Al}}$  or vice versa. Hence, the solubility product, at least heuristically, arises from the coupling that occurs between the concentration in solution and the distribution of surface sites. Note that it is the crystal structure itself which couples the effects. The surface couples the concentrations because the arrival of atoms of a given type can influence both the local bonding of atoms of different types, as well as the number of available sites for other types of atoms to attach themselves to the surface. To proceed further and truly quantify the coupling and understand the kinetic justification for the employment of a solubility product, we need a quantitative analysis of the proper kinetic mechanism that fully incorporates the correlation between the kinetics of neighboring sites via all the changes in bonding.<sup>16,21</sup>

### Deriving a Kinetic Solubility Product from a Comprehensive Theory Feldspar Model

Feldspar, an aluminosilicate, is the most common mineral in the earth’s crust.<sup>22</sup> It consists of a tectosilicate tetrahedral framework involving Si–O–Si and Si–O–Al linkages with alkalis or alkaline earth cations balancing charge in the interstices or “cages” of the framework. Feldspar dissolution is of great geochemical interest and has been extensively studied experimentally.<sup>22</sup> It provides an important test of our understanding of the origin of  $\Delta G$  in the kinetic model. If the case of albite dissolution is taken into account, the reaction at equilibrium could be written as eq 5



$$K'_{\text{sp}} = a_{\text{Na}^+} a_{\text{Al}(\text{OH})_4^-} a_{\text{H}_4\text{SiO}_4}^3 \quad (5\text{B})$$

setting  $a_{\text{H}_2\text{O}} = 1$ .  $K'_{\text{sp}}$  is the solubility product. The equilibrium eq 5B relates the concentration of the species in a highly nonlinear fashion. In nonequilibrium situations, we then compare the solubility product to  $K'_{\text{sp}}$ , and many studies introduce the term as in eq 6

$$1 - Q = 1 - \frac{a_{\text{Na}^+} a_{\text{Al}(\text{OH})_4^-} a_{\text{H}_4\text{SiO}_4}^3}{K_{\text{eq}}} = K'_{\text{sp}} \quad (6)$$

to calculate rates.<sup>7</sup> No current kinetic theory of water–rock interactions is capable of deriving (not assuming) the origin of the relation (eq 5B) in the rate law from the various separate kinetic basic processes (attachments, detachments, diffusion, etc.) that are constantly taking place between a mineral surface and a fluid, because the assumed reaction mechanisms are too limited. Certainly, models that focus on one or several surface “complexes” with or without the presence of ligands and that do not even consider the role of “kink sites” or steps in mineral structures cannot possibly explain why eq 5B arises from the kinetic processes. Instead, these “molecular” approaches just attach a  $\Delta G$  dependence to any discussion of the rate, usually quoting some results from elementary reactions or chains of elementary reactions (see discussion in ref 23).

To illustrate the new kinetic thinking further, we will introduce a simple “feldspar” model here and use the concepts in ref 16 to then explain precisely how and why the solubility product arises once a crystal-based kinetic reaction mechanism is used. To make matters relatively simple, the 3D four-coordinated tetrahedral feldspar framework (omitting alkalis) will be projected onto a 2D-layer model, and we will study how growth or dissolution of this feldspar-like layer justifies a solubility product, not from thermodynamics, but from kinetics.

Figure 1 exhibits the crystal structure. The structure stoichiometry can be readily checked to be that of  $\text{AlSi}_3$ . Both Si and Al have four neighbors (i.e., they possess tetrahedral coordination). The Al atoms are ordered so that no Al–Al neighboring pairs are allowed. Note that the usual oxygen bridges have been omitted for simplicity, but each Al–Si bonding pair represents an Al–O–Si bond and each Si–Si bonding pair a Si–O–Si bond. Figure 1A has been drawn to also give rise to a highly reactive surface (or *K*-face). In a four-coordinated bulk structure, “kinks” are atoms with two neighbors.<sup>2</sup> All the atoms on the very reactive surface in Figure 1A are kinks. Thus, as Si and Al atoms arrive at the surface, they are readily incorporated into the structure (two bonds hold them much better than the usual one bond for adatoms). As a result, the surface expands quickly in a manner similar to that shown in Figure 1B. These protuberances will move until terminated by single atoms (similar to a stack of blocks). The *K*-surface is quickly becoming bound by much less reactive (near equilibrium) *F*-faces, the usual surfaces of euhedral crystals.<sup>6</sup> These euhedral faces grow by the movement of steps. If we focus on the *F*-face limiting the growth (or dissolution) in Figure 1B, we obtain the *F*-face in Figure 1C.

The point is that, as equilibrium is approached, steps on euhedral faces begin to take over as the mechanism of dissolution or growth (see discussion in refs 16 and 21, where this change of mechanism has been shown to even produce stair-like steps on the dissolution rate variation as a function of saturation state due to a switch over between step motion and a hole-nucleation mechanism). Figure 1C displays a step with an Al kink. Note that now the step atoms have higher bonding

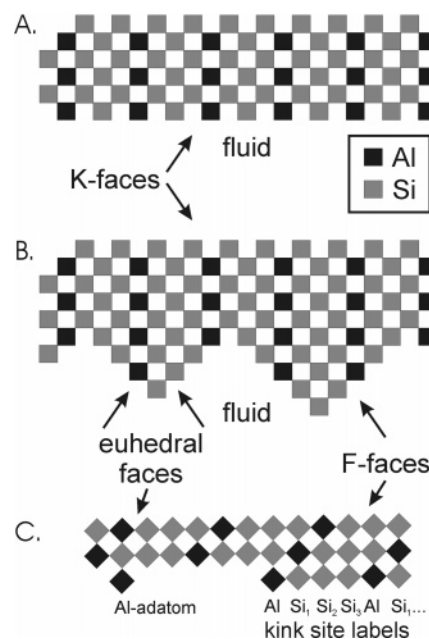


**Figure 1.** (A) Simplified model of a feldspar surface. The four-coordinated framework has been “squashed” into two dimensions. Note the  $\text{AlSi}_3$  stoichiometry. The “face” shown is a reactive surface or *K*-face with all sites bonding new additions via two bonds. (B) Surface in (A) after reaction with a fluid. The reactive sites grow (or dissolve) quickly to produce protuberances bounded by slow euhedral faces (*F*-faces). (C) A euhedral face (*F*-face) of our “crystal”, which grows or dissolves in an orderly step-controlled fashion. An Al kink site is shown. Note the different kink sites produced by the removal of the Al kink atom and subsequent Si atoms along the step. These kink sites will be labeled Al, Si<sub>1</sub>, Si<sub>2</sub>, and Si<sub>3</sub> in the text.

( $n = 3$ ) and that any atom arriving on a step (not a kink) will only attach by one bond to the surface, producing an adatom. Thus, the arrival via random collision processes at the kink sites is much favored over arrival at steps. Similarly, departures from kink sites is much favored over departures of the highly bonded step sites. As carried out in ref 16, we now want to analyze the situation with the reactive kink sites (where attachment leads to  $n = 2$ ). Removing or adding a kink atom will produce another kink atom. If one successively removes the kink Al atom and the subsequent Si atoms along the dissolving step, it is clear that there are four types of kink sites in our “feldspar” structure: one Al kink site and three Si kink sites, labeled as Si<sub>1</sub>, Si<sub>2</sub>, and Si<sub>3</sub> in Figure 1C. It is the dynamics of these kink sites that will enter into the formulation of the overall rate law.

The first step is to establish the kinetic equations for the number of kinks,  $N_{\text{Al}}^k$ ,  $N_{\text{Si}_1}^k$ ,  $N_{\text{Si}_2}^k$ , and  $N_{\text{Si}_3}^k$ , similar to the treatment done in ref 16. The equation for  $N_{\text{Al}}^k$  is given by eq 7

$$\frac{dN_{\text{Al}}^k}{dt} = k_{\text{Al}}^+ N_{\text{Si}_1}^k + k_{\text{Si}_3}^- N_{\text{Si}_3}^k - k_{\text{Al}}^- N_{\text{Al}}^k - k_{\text{Si}_1}^+ N_{\text{Al}}^k \quad (7)$$

The first term is the rate of arrival of Al atoms at Si<sub>1</sub> kink sites, thereby producing an Al kink. Si<sub>1</sub> kink sites are the only kink sites where Al atoms can attach in the structure (Figure 1C).  $k_{\text{Al}}^+$  is the attachment rate constant for Al atoms from solution (which depends on  $C_{\text{Al}}$ , see following text). The second term is the removal rate of Si atoms from an Si<sub>3</sub> kink site. Each Si atom removed from a Si<sub>3</sub> kink site produces an Al kink site (Figure 1C).  $k_{\text{Si}_3}^-$  is the rate constant for the removal of one Si atom from a Si<sub>3</sub> kink site. The third term is the rate of removal of Al atoms from Al kink sites.  $k_{\text{Al}}^-$  is the rate constant for Al



removal from an Al kink site. Finally, the fourth term is the addition of Si atoms at Al kink sites, thereby producing an Si<sub>3</sub> kink site and removing an Al kink site.  $k_{\text{Si}}^+$  is the attachment rate constant for Si atoms from solution, which again is a function of  $C_{\text{Si}}$  in solution (see following text). It is important to note that, because the Si and Al species collide with the surface from a homogeneous solution, there is only one  $k_{\text{Al}}^+$  and one  $k_{\text{Si}}^+$ , which depend on the solution concentrations of  $C_{\text{Al}}$  and  $C_{\text{Si}}$ , respectively. We will return to these rate constants later.

In a similar manner, one can write down the various processes which affect the number of kinks for sites Si<sub>1</sub>, Si<sub>2</sub>, and Si<sub>3</sub>. For  $N_{\text{Si}_1}^k$ , eq 8 is

$$\frac{dN_{\text{Si}_1}^k}{dt} = k_{\text{Si}}^+ N_{\text{Si}_2}^k + k_{\text{Al}}^- N_{\text{Al}}^k - k_{\text{Si}_1}^- N_{\text{Si}_1}^k - k_{\text{Al}}^+ N_{\text{Si}_1}^k \quad (8)$$

The first two terms reflect that adding an Si to an Si<sub>2</sub> kink site produces an Si<sub>1</sub> kink (Figure 1C) and that removing an Al from an Al kink site also produces a Si<sub>1</sub> kink. The third and fourth terms reflect that removing an Si from an Si<sub>1</sub> site or adding an Al to an Si<sub>1</sub> kink site both reduce the number of Si<sub>1</sub> kink sites. Likewise, the rate equations for the other kink sites are

$$\frac{dN_{\text{Si}_2}^k}{dt} = k_{\text{Si}}^+ N_{\text{Si}_3}^k + k_{\text{Si}_1}^- N_{\text{Si}_1}^k - k_{\text{Si}_2}^- N_{\text{Si}_2}^k - k_{\text{Si}}^+ N_{\text{Si}_2}^k \quad (9)$$

$$\frac{dN_{\text{Si}_3}^k}{dt} = k_{\text{Si}}^+ N_{\text{Al}}^k + k_{\text{Si}_2}^- N_{\text{Si}_2}^k - k_{\text{Si}_3}^- N_{\text{Si}_3}^k - k_{\text{Si}}^+ N_{\text{Si}_3}^k \quad (10)$$

These four eqs (7–10) can be used to solve for the number,  $N_i^k$ , of the various kink sites, if steady state is assumed (i.e.,  $dN_i^k/dt = 0$ ). Actually, because as can be checked from adding eqs 7–10, eq 11

$$\frac{dN_{\text{Al}}^k}{dt} + \frac{dN_{\text{Si}_1}^k}{dt} + \frac{dN_{\text{Si}_2}^k}{dt} + \frac{dN_{\text{Si}_3}^k}{dt} = 0 \quad (11)$$

one of the four equations is a dependent equation. Equation 11 merely states that the total number of kink sites is basically constant in the process and, in fact, given from statistical mechanics as discussed in ref 16. Therefore, one can solve for the ratios:  $N_i^k/N_{\text{Al}}^k$ . If we label the ratios as  $X_1 \equiv N_{\text{Si}_1}^k/N_{\text{Al}}^k$ ,  $X_2 \equiv N_{\text{Si}_2}^k/N_{\text{Al}}^k$ , and  $X_3 \equiv N_{\text{Si}_3}^k/N_{\text{Al}}^k$ , then dividing eq 7 by  $N_{\text{Al}}^k$  and setting it equal to zero, we obtain eq 12:

$$k_{\text{Al}}^+ X_1 + k_{\text{Si}_3}^- X_3 = \text{Al}^- + k_{\text{Si}}^+ \quad (12)$$

Similarly, dividing eq 8 by  $N_{\text{Al}}^k$  and setting it equal to zero yields

$$-(k_{\text{Si}_1}^- + k_{\text{Al}}^+) X_1 + k_{\text{Si}_2}^+ X_2 = -k_{\text{Al}}^- \quad (13)$$

and using eq 10 divided by  $N_{\text{Al}}^k$  and setting it equal to zero produces eq 14:

$$k_{\text{Si}_2}^- X_2 - (k_{\text{Si}_3}^- + k_{\text{Si}}^+) X_3 = -k_{\text{Si}}^+ \quad (14)$$

We can solve these equations for  $X_i$  fairly straightforwardly, because eqs 12–14 are linear equations. The results are eqs 15–17:

$$X_1 = \frac{N_{\text{Si}_1}^k}{N_{\text{Al}}^k} = \frac{k_{\text{Si}}^{+2}(k_{\text{Si}}^+ + k_{\text{Al}}^-) + k_{\text{Si}_3}^- k_{\text{Al}}^-(k_{\text{Si}}^+ + k_{\text{Si}_2}^-)}{D} \quad (15)$$

$$X_2 = \frac{N_{\text{Si}_2}^k}{N_{\text{Al}}^k} = \frac{k_{\text{Si}}^{+2}(k_{\text{Al}}^+ + k_{\text{Si}_1}^-) + k_{\text{Al}}^- k_{\text{Si}_1}^-(k_{\text{Si}}^+ + k_{\text{Si}_3}^-)}{D} \quad (16)$$

$$X_3 = \frac{N_{\text{Si}_3}^k}{N_{\text{Al}}^k} = \frac{k_{\text{Si}}^+ k_{\text{Al}}^-(k_{\text{Si}}^+ + k_{\text{Si}_2}^-) + k_{\text{Si}_1}^- k_{\text{Si}_2}^-(k_{\text{Si}}^+ + k_{\text{Al}}^-)}{D} \quad (17)$$

where eq 18

$$D \equiv k_{\text{Si}}^+ k_{\text{Al}}^-(k_{\text{Si}}^+ + k_{\text{Si}_3}^-) + k_{\text{Si}_2}^- k_{\text{Si}_3}^-(k_{\text{Al}}^+ + k_{\text{Si}_1}^-) \quad (18)$$

Having established the steady-state values of  $N_i^k$ , we are now in a position to calculate the overall dissolution rate in a manner similar to that in ref 16. The overall dissolution rate can be obtained from the net difference between attachment and detachment of the various atoms to the surface kink sites. Again, using Figure 1C, we see that Si and Al atoms can attach at the appropriate kink sites and also detach from each Si or Al kink site. Therefore, one can readily write for the overall rate of dissolution eq 19:

$$\text{Overall Dissolution Rate} = k_{\text{Al}}^- N_{\text{Al}}^k + k_{\text{Si}_1}^- N_{\text{Si}_1}^k + k_{\text{Si}_2}^- N_{\text{Si}_2}^k + k_{\text{Si}_3}^- N_{\text{Si}_3}^k - k_{\text{Al}}^+ N_{\text{Si}_1}^k - k_{\text{Si}}^+(N_{\text{Al}}^k + N_{\text{Si}_2}^k + N_{\text{Si}_3}^k) \quad (19)$$

It is important to note that, because the Si and Al species collide with the surface from a homogeneous solution, there is only one  $k_{\text{Al}}^+$  and one  $k_{\text{Si}}^+$ , which depend on the solution concentration  $C_{\text{Al}}$  and  $C_{\text{Si}}$ , respectively. We will return to these rate constants later. Dividing the rate by  $N_{\text{Al}}^k$  and multiplying by the denominator,  $D$ , we can rewrite eq 19 as eq 20

$$\frac{D}{N_{\text{Al}}^k} \text{Rate} = (k_{\text{Al}}^- - k_{\text{Si}}^+) D + (k_{\text{Si}_1}^- - k_{\text{Al}}^+) \left( \frac{N_{\text{Si}_1}^k}{N_{\text{Al}}^k} \right)^{\text{num}} + (k_{\text{Si}_2}^- - k_{\text{Si}}^+) \left( \frac{N_{\text{Si}_2}^k}{N_{\text{Al}}^k} \right)^{\text{num}} + (k_{\text{Si}_3}^- - k_{\text{Si}}^+) \left( \frac{N_{\text{Si}_3}^k}{N_{\text{Al}}^k} \right)^{\text{num}} \quad (20)$$

where the num superscript denotes using only the numerators of the expressions in eqs 15–17. At this point, if one multiplies out the terms on the right side of eq 20 (using the numerators in eqs 15–17), the result will be seen to lead to a large number of cancellations, leaving behind only eight terms, four of which are the same. Therefore, eq 20 leads immediately to eq 21:

$$\frac{D}{N_{\text{Al}}^k} \text{Rate} = 4(k_{\text{Al}}^- k_{\text{Si}_1}^- k_{\text{Si}_2}^- k_{\text{Si}_3}^- - k_{\text{Si}}^{3+} k_{\text{Al}}^+) \quad (21)$$

To finish the analysis, we must discuss the actual rate constants involved in eq 21. Let us label  $\Phi_{\text{SiSi}}$  and  $\Phi_{\text{SiAl}}$  the energy changes needed to rupture an Si–O–Si and an Si–O–Al bond, respectively. Then, because an Al atom in an Al kink site has two Si–O–Al bonds (Figure 1C), the detachment rate,  $k_{\text{Al}}^-$ , is given by eq 22

$$k_{\text{Al}}^- = \nu_1 e^{-2\Phi_{\text{SiAl}}/kT} \quad (22)$$

where  $\nu_1$  is a frequency parameter, related to the time scale and, in general, obtainable from experiment.<sup>16,17</sup> Similarly, on

the basis of the bonding in Figure 1C, Si<sub>1</sub> and Si<sub>3</sub> kink sites have one Si–O–Si and one Si–O–Al bond, so that eq 23 is

$$k_{\text{Si}_1}^- = k_{\text{Si}_3}^- = \nu_2 e^{-\Phi_{\text{SiSi}}/kT} e^{-\Phi_{\text{SiAl}}/kT} \quad (23)$$

Finally, Si<sub>2</sub> sites have two Si–O–Si bonds, so that eq 24 is

$$k_{\text{Si}_2}^- = \nu_3 e^{-2\Phi_{\text{SiSi}}/kT} \quad (24)$$

In most of our modeling and exploration of the kinetic dissolution mechanism, we have set  $\nu_1 = \nu_2 = \nu_3 = \nu$ .<sup>17</sup> However, in practice, there can be differences in the  $\nu$ 's. They still must be bounded by the experimental rate constant as illustrated in ref 17.

At this point, we need to discuss the attachment rates,  $k_{\text{Si}}^+$  and  $k_{\text{Al}}^+$ . As discussed in ref 2, the Si and Al attachment rates depend on the average kink site in the mineral structure, as well as on the solution concentration. Because all Al atoms have four Si neighbors in the bulk, the average kink site has two Al–O–Si bonds, so eq 25 is

$$k_{\text{Al}}^+ = \nu_1 e^{-2\Phi_{\text{SiAl}}/kT} e^{\Delta\mu_{\text{Al}}/kT} \quad (25)$$

Equation 22 is such that, at equilibrium with respect to Al (i.e.,  $\Delta\mu_{\text{Al}} = 0$ , or  $C_{\text{Al}} = C_{\text{Al,eq}}$ ), the arrival rate,  $k_{\text{Al}}^+$ , matches departures from the average Al kink site, on the basis of the bulk structure.<sup>2</sup> For nonequilibrium values of  $C_{\text{Al}}$ , then the rate in eq 25 varies linearly with  $C_{\text{Al}}$ , on the basis of the thermodynamic identity of eq 26:

$$\frac{C_{\text{Al}}}{C_{\text{Al,eq}}} = e^{\Delta\mu_{\text{Al}}/kT} \quad (26)$$

$C_{\text{Al,eq}}$  is calculated from the stoichiometric dissolution; that is, if

$$C_{\text{Al,eq}} C_{\text{Si,eq}}^3 = K_{\text{sp}}$$

where  $K_{\text{sp}}$  would include the ionic strength and sodium or potassium concentration in eq 5B (i.e.,  $K_{\text{sp}} = K'_{\text{sp}}/a_{\text{Na}^+}\gamma_{\text{Al}}\gamma_{\text{Si}}^3$ ), then from stoichiometry, eq 27 is

$$C_{\text{Al,eq}} = 1/3 C_{\text{Si,eq}} = (K_{\text{sp}}/27)^{1/4} \quad (27)$$

There are two types of Si in this structure. Two-thirds of the Si atoms have two Si neighbors and two Al neighbors (see Figure 1A), while one-third of the Si atoms in the bulk have four Si neighbors. Therefore, the average number of Si neighbors of an Si atom in the bulk is  $2/3 \times 2 + 1/3 \times 4$  or  $8/3$ Si, and the average number of Al neighbors is  $2/3 \times 2 + 1/3 \times 0$  or  $4/3$ Al. Hence, the average Si kink has  $4/3$  Si–O–Si bonds and  $2/3$  Si–O–Al bonds. By our treatment, the attachment rate depends then on the detachment rate of this average Si kink and on the concentration of Si in solution ( $\Delta\mu_{\text{Si}}$ ). Therefore, eq 28 follows

$$k_{\text{Si}}^+ = \nu^+ e^{-(4/3)\Phi_{\text{SiSi}}/kT} e^{-(2/3)\Phi_{\text{SiAl}}/kT} e^{\Delta\mu_{\text{Si}}/kT} \quad (28)$$

But, note that, on the basis of eqs 23 and 24, our general equation for  $k_{\text{Si}}^+$  also can be written as eq 29

$$k_{\text{Si}}^+ = (k_{\text{Si}_1}^- k_{\text{Si}_2}^- k_{\text{Si}_3}^-)^{1/3} e^{\Delta\mu_{\text{Si}}/kT} \quad (29)$$

if  $\nu^+ = (\nu_2^2 \nu_3)^{1/3}$ , so that  $k_{\text{Si}}^+$  depends on the geometric mean of the  $k_{\text{Si}_i}^-$ . Inserting eqs 25 and 29 into the equation for the

overall rate (eq 21), we obtain eq 30:

$$\text{Rate} = \frac{4N_{\text{Al}}^k}{D} k_{\text{Al}}^- k_{\text{Si}_1}^- k_{\text{Si}_2}^- k_{\text{Si}_3}^- (1 - e^{3\Delta\mu_{\text{Si}}/kT} e^{\Delta\mu_{\text{Al}}/kT}) \quad (30)$$

Even though  $k_{\text{Al}}^+$  and  $k_{\text{Si}}^+$  do depend only on  $C_{\text{Al}}$  and  $C_{\text{Si}}$  individually (e.g., see eqs 25 and 28), eq 30 has accomplished the crucial link between the overall kinetic model and thermodynamics. When the interactions between the kink sites on the surface and the bonding are all taken into account, the overall rate does indeed depend not on  $k_{\text{Al}}^+$  and  $k_{\text{Si}}^+$  independently, but on the composite quantity

$$(1 - e^{3\Delta\mu_{\text{Si}}/kT} e^{\Delta\mu_{\text{Al}}/kT})$$

which could also be written using eq 26 as

$$\left(1 - \frac{C_{\text{Si}}^3 C_{\text{Al}}}{C_{\text{Si,eq}}^3 C_{\text{Al,eq}}}\right)$$

or using eq 27 as

$$\left(1 - \frac{C_{\text{Si}}^3 C_{\text{Al}}}{K_{\text{sp}}}\right)$$

This final term has recaptured the solubility product. The coupling of all the various individual arrival and departure rates for Al and Si atoms via the kink sites in the crystal structure has led to a nonlinear  $C_{\text{Si}}^3 C_{\text{Al}}$  dependence of the Rate.

Note that acknowledging a major role for the solubility product demands that even in dissolution there must be numerous bond-forming reactions taking place; that is, both the forward and reverse reactions of hydrolysis, including  $\text{H}^+$ ,  $\text{OH}^-$ , or organic-ligand-promoted hydrolysis, must be included in the dissolution kinetic reaction mechanism. This inclusion of bond formation in the kinetics is a necessity, but it has far-reaching implications to the concept of how dissolution really takes place, as discussed at length in ref 16.

If we write  $\Delta G = 3\Delta\mu_{\text{Si}} + \Delta\mu_{\text{Al}}$ , then the rate law takes the usual form

$$\text{Rate} = \frac{4N_{\text{Al}}^k}{D} k_{\text{Al}}^- k_{\text{Si}_1}^- k_{\text{Si}_2}^- k_{\text{Si}_3}^- (1 - e^{\Delta G/RT})$$

We can rewrite this expression in a more general way, using the expression for the total number of kinks on the surface,  $N_{\text{tot}}^k$

$$\begin{aligned} N_{\text{tot}}^k &= N_{\text{Al}}^k + N_{\text{Si}_1}^k + N_{\text{Si}_2}^k + N_{\text{Si}_3}^k \\ &= N_{\text{Al}}^k (1 + X_1 + X_2 + X_3) \end{aligned}$$

Using eqs 15–17 for  $X_i$ , we get eq 31

$$N_{\text{tot}}^k = \frac{N_{\text{Al}}^k}{D} S \quad (31)$$

and eq 32 defines  $S$  as

$$\begin{aligned} S &= 2k_{\text{Si}}^{+3} + 2k_{\text{Si}}^{+2} k_{\text{Al}}^+ + k_{\text{Si}}^{+2} (k_{\text{Al}}^- + k_{\text{Si}_1}^-) + k_{\text{Si}}^+ k_{\text{Al}}^+ (k_{\text{Si}_2}^- + k_{\text{Si}_3}^-) + \\ &+ k_{\text{Si}}^+ (k_{\text{Al}}^- k_{\text{Si}_1}^- + k_{\text{Si}_1}^- k_{\text{Si}_2}^- + k_{\text{Al}}^- k_{\text{Si}_3}^-) + k_{\text{Al}}^+ k_{\text{Si}_2}^- k_{\text{Si}_3}^- + k_{\text{Al}}^- (k_{\text{Si}_1}^- k_{\text{Si}_2}^- + \\ &+ k_{\text{Si}_1}^- k_{\text{Si}_3}^- + k_{\text{Si}_2}^- k_{\text{Si}_3}^-) + k_{\text{Si}_1}^- k_{\text{Si}_2}^- k_{\text{Si}_3}^- \quad (32) \end{aligned}$$

If we use eq 31, our final expression for the overall rate becomes eq 33:

$$\text{Rate} = N_{\text{tot}}^k \frac{4}{S} k_{\text{Al}}^- k_{\text{Si}_1}^- k_{\text{Si}_2}^- k_{\text{Si}_3}^- (1 - e^{\Delta G/RT}) \quad (33)$$

The importance of the  $\Delta G$  term in our final eq 33, of course, is that it clearly shows that  $\Delta\mu$  or  $\Delta G$  controls the rate as equilibrium is approached, such that the  $\text{Rate} \rightarrow 0$  as  $\Delta G \rightarrow 0$ . Nonetheless, as solution conditions deviate from equilibrium, we need to establish how other factors such as  $N_{\text{tot}}^k$  vary, how diffusion affects the rate, and also, very crucially, how steps themselves may be generated.<sup>4,5,19,20</sup> The latter problem has led to the treatment of stepwaves emanating from dislocation etch pits.<sup>4,5</sup> This implies very nonlinear rate laws, as verified by refs 19 and 20. In addition, as higher undersaturations are reached, we need to worry about nonstep mechanisms, as already shown in ref 21. All these factors can lead to modifications in the  $\Delta G$  term (i.e., terms such as  $(1 - e^{\alpha\Delta G/kT})$ ,  $\alpha$  small, or the  $(1 - e^{\Delta G/kT})^n$ -type curves ( $n > 1$ )).<sup>17</sup> The precise  $\Delta G$  variation can be analyzed by the complete dissolution mechanism as introduced by ref 17. Nevertheless, eq 33 incorporates many factors that heretofore did not have an adequate approach to be treated simultaneously. In particular, eq 33 can provide a unifying link not only to the presence of  $\Delta G$  (or the solubility product) in the rate but also to the handling of inhibition and the justification for the so-called product-type rate laws often used by experimentalists.<sup>23</sup>

### Overall Rate Law and Inhibition

Inhibition effects have been observed in a variety of experimental work. In particular, the concentration of Al in solution has been shown to inhibit the rate of feldspar dissolution.<sup>24,25</sup> Earlier papers<sup>16,17</sup> have discussed these inhibition effects from the point of view of the general kinetic model. Equation 33 can be used to provide a more succinct insight into how these effects emerge from the surface dynamics during dissolution. Specifically, it would be illuminating to verify that for the “feldspar” case (a) Si concentration does little to inhibit the rate and that (b) Al concentration does inhibit the rate in a roughly  $1/C_{\text{Al}}^n$  fashion, where  $n$  is small ( $n < 1$ ). Of course, other structures can exhibit many variations depending on the full reaction mechanism.<sup>16</sup> If at higher undersaturations  $N_{\text{tot}}^k$  approaches a limiting value,<sup>16</sup> then the  $S$  term can indeed account for both of these observations. If we vary  $C_{\text{Si}}$  far from equilibrium, then we set  $\Delta\mu_{\text{Al}} \ll 0$ , so that  $k_{\text{Al}}^+ \rightarrow 0$  (e.g., eq 25). In this case, the  $S$  term (eq 32) behaves as eq 34

$$S = 2k_{\text{Si}}^{3+} + Ak_{\text{Si}}^{2+} + Bk_{\text{Si}}^{+} + C \quad (34)$$

where

$$A = k_{\text{Al}}^- + k_{\text{Si}_1}^-; \quad B = k_{\text{Al}}^- k_{\text{Si}_1}^- + k_{\text{Si}_1}^- k_{\text{Si}_2}^- + k_{\text{Al}}^- k_{\text{Si}_3}^-$$

and

$$C = k_{\text{Al}}^- (k_{\text{Si}_1}^- k_{\text{Si}_2}^- + k_{\text{Si}_1}^- k_{\text{Si}_3}^- + k_{\text{Si}_2}^- k_{\text{Si}_3}^-) + k_{\text{Si}_1}^- k_{\text{Si}_2}^- k_{\text{Si}_3}^-$$

The variation of the dissolution rate of feldspars with varying Al/Si ratios<sup>26,27</sup> clearly shows that the Al–O–Si bond breaks at least an order of magnitude faster than the Si–O–Si bond at temperatures of 25 to 200 °C. Therefore,  $\Phi_{\text{SiAl}} < \Phi_{\text{SiSi}}$  by several kilocalories per mole. However, because  $\Phi_{\text{SiAl}} < \Phi_{\text{SiSi}}$ , all the terms involving  $k_{\text{Si}}^+$  and  $k_{\text{Si}}^-$  are much smaller than  $k_{\text{Al}}^-$

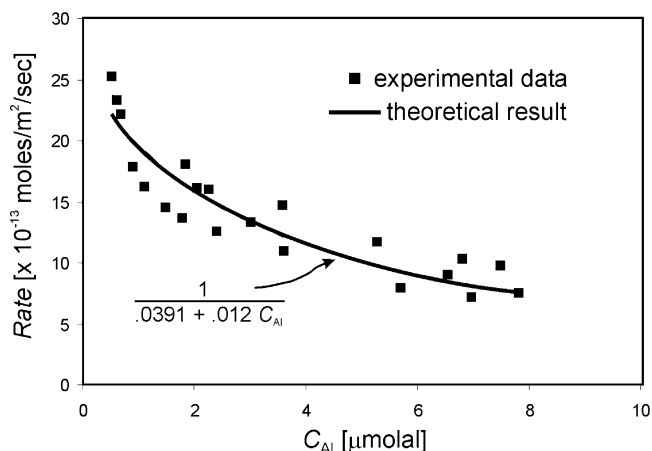


**Figure 2.** Rate vs aluminum concentration,  $C_{\text{Al}}$ , plot comparing experimental data by Gautier et al.<sup>25</sup> with our theoretical rate law (see text).

(compare eqs 22 and 25 to eqs 23, 24, and 28). In fact, because of the disparity in  $\Phi$  values,  $k_{\text{Al}}^- \gg k_{\text{Si}_1}^- = k_{\text{Si}_3}^- \gg k_{\text{Si}_2}^- > k_{\text{Si}_1}^+$ , and so, the biggest term in  $S$  (eq 32) is the  $k_{\text{Al}}^- k_{\text{Si}_1}^- k_{\text{Si}_3}^-$  term in  $C$ . As a result, the  $C$  term dominates the other terms in eq 34, and varying  $k_{\text{Si}}^+$  will not change the magnitude of  $S$  much. Consequently, variations in  $C_{\text{Si}}$  will have little effect on the overall rate far from equilibrium, as observed.

On the other hand, if we vary  $C_{\text{Al}}$  far from equilibrium, then we set  $\Delta\mu_{\text{Si}} \ll 0$  so that  $k_{\text{Si}}^+ \rightarrow 0$ . Under these conditions, the  $S$  term can be written as eq 35

$$S = A'k_{\text{Al}}^{+} + C \quad (35)$$

where  $A' = k_{\text{Si}_2}^- k_{\text{Si}_3}^-$  and  $C$  is the same as in eq 34. However, now the term containing the  $k_{\text{Al}}^{+}$  term is comparable to terms such as  $k_{\text{Al}}^- k_{\text{Si}_1}^- k_{\text{Si}_3}^-$  in  $C$ . Therefore, there should be an increase in  $S$  as  $k_{\text{Al}}^{+}$  increases and accordingly an Al concentration inhibition effect. Of course, because of the presence of the  $C$  term in eq 35, the dependence of  $S$  on  $C_{\text{Al}}$  leads to a rate variation that is less than  $1/C_{\text{Al}}$ . In fact, on the basis of eq 33, the rate varies as  $1/(A'k_{\text{Al}}^{+} + C)$  in this case, which will lead to an inhibitory effect roughly more like  $1/C_{\text{Al}}^n$  where  $n < 1$ , as is in fact observed.<sup>25</sup> Note that eq 33 not only predicts inhibition by  $C_{\text{Al}}$  but also the lack of such for  $C_{\text{Si}}$  in accordance with experimental data; however, for high enough  $C_{\text{Si}}$  there could be inhibition arising from  $C_{\text{Si}}$ . This asymmetry is different<sup>1</sup> from the inhibition found for AB crystals in ref 16. As an application of eqs 33 and 35, the data for Al inhibition of the  $K$ -feldspar dissolution rate of Gautier et al.<sup>25</sup> can be analyzed. By the utilization of all rates obtained for the conditions of  $\Delta G < -40$  kJ/mole ( $-9.6$  kcal/mol) and with  $C_{\text{Al}} < 1 \times 10^{-5}$  molal (i.e., “far from equilibrium”), the Rate versus  $C_{\text{Al}}$  data do conform nicely to the expected rate law

$$\text{Rate} = \frac{10^{-13}}{0.0391 + 0.012C_{\text{Al}}} \text{ mol/m}^2 \text{ sec}$$

within the uncertainty of the experimental data (see Figure 2).

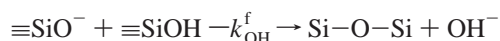
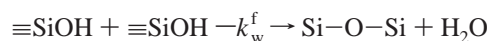
### Ph Effects and Product Rate Laws

Many researchers have employed rate laws such as eq 36

$$\text{Rate} = k_0 A e^{-E/RT} a_{\text{H}^+}^n g(I) (1 - e^{\Delta G/RT})^n \quad (36)$$

where  $E$  is the overall activation energy,  $A$  is the surface area,

and where the pH effects ( $a_{H^+}$  term), the inhibition effects ( $g(I)$ ), and the saturation-state effect ( $\Delta G$ ) are all multiplied.<sup>8,23</sup> Values of  $n \neq 1$  have originated mainly from reaction mechanisms involving defects, such as the BCF growth mechanism.<sup>2,6</sup> Equation 30 can now begin to provide a fundamental justification for these previous phenomenological rate laws. Note that eq 33 indeed multiplies a term  $k_{Al}^- k_{Si_1}^- k_{Si_2}^- k_{Si_3}^-$  by a saturation-state term combining the dynamics of all the species. Interestingly, there are four terms all multiplied together and affecting the rate in front of eq 33. However, we also have division by the  $S$  term. Because the large terms in  $S$  are the  $k_{Al}^-$  terms,  $k_{Al}^-$  largely cancels between denominator and the four-term product. Therefore, the magnitude of the rate as well as the pH effect (or ligand effects) will be determined mostly by the slow Si detachment rate constants. pH or ionic strength effects enter dominantly via their effect on  $k_i^-$ , which are multiplying the rate in eq 33. And so, these effects will also lead, using eq 33, to a product-like rate law. pH effects can be readily understood within the full-dimensional crystal reaction mechanism of ref 2. The presence of  $H^+$  or  $OH^-$  in solution will lower the energy change needed to rupture the Si—O—Si (or Si—O—Al) bonds, leading to a shift in the ratio of the number of broken bonds to the number of formed bonds in the mineral surface (e.g., ref 19). This shift will lead to an effective lowering of  $\Phi_{SiSi}$  and  $\Phi_{SiAl}$ . Thus,  $k_{Si}^-$  will also vary with the drop in  $\Phi_{SiSi}$  as shown in eqs 23 and 24. To quantify this change, one needs to analyze the change in energy upon rupturing the Si—O—Si bond in the presence of water ( $\Delta E_w$ ), the change in energy upon hydrolizing the Si—O—Si bond with  $OH^-$  ( $\Delta E_{OH}$ ), and the ratio of the elementary rate constants  $k_{OH}^f/k_w^f$  for the formation of the Si—O—Si bond in the presence of  $OH^-$  and  $H_2O$ , or the rate constants for the reactions



However, it can be said that, while the relationship between  $k_{Al}^-$ ,  $k_{Si}^-$ , and so on, and  $X_{H^+,ads}$  or  $X_{OH^-,ads}$  is nontrivial, in many instances it does reduce within a good approximation to eq 37

$$k_{Si_i}^- \cong k_{Si_i}^{-o} X_{H^+} \quad \text{or} \quad k_{Si_i}^- \cong k_{Si_i}^{-o} X_{OH^-}, \text{ ads} \quad (37)$$

which has been implicit in many experimental results.<sup>8,28</sup> Note that, if indeed the  $k_{Si_i}^-$  values are approximately linearly proportional to  $X_{H^+,ads}$  or  $X_{OH^-,ads}$ , then the ratio of the four-term product and the three-term products in the  $S$  term in eq 33 will yield overall rates that will also vary linearly in approximately the same manner. In short, the form of eq 33 where the  $S$  term and the four-rate-constant  $k^-$  term are multiplied by the  $f(\Delta G)$  term explains the success of models that multiply inhibitory effects and pH effects with  $\Delta G$  effects. The main result that we want to emphasize here is that, from the form of eq 33, one can indeed expect that phenomenological rate laws such as in eq 37 should provide an adequate representation of the full rate law. We had no previous accounting for such rate laws, except as reasonable and useful approaches to treat experimental data. Equation 32 indicates that there is a more profound reason for the multiplicative phenomenological rate law.

## Conclusions

This paper has extended the general kinetic approach introduced in refs 16, 17, and 21 to understand the underpinning

of critical kinetic parameters such as the solubility product, or  $\Delta G$ , as well as inhibition and the product-type rate laws for a more complex structure, such as a feldspar-like model. The kinetic treatment can indeed justify the use of a nonlinear solubility product even in a kinetic model that has the arrival and departure of molecular units independently controlled by their respective concentration in solution and their bonding on the surface. The reason for the appropriateness of  $\Delta G$  in a rate law stems from the bonding interrelations that arise between the neighboring units at the surface because of the crystal structure. Therefore, the surface bonding relationships lead to a coupling of the arrival and departures in such a way that only the solubility product controls the overall rate and not the individual species rate constants (or concentrations).

The derivation of the central role played by the solubility product required a kinetic model that can handle the three-dimensional nature of the dissolution process as well as the many-body aspects of the kinetics, which has been already emphasized in refs 16 and 21. In addition, the role of steps and, in particular, kink sites along surface steps needed to be carefully analyzed to obtain the  $\Delta G$  dependence. As part of the analysis, the necessity to include bond formation along with bond rupture was another fundamental concept in the treatment of the kinetic mechanism. The entire development, therefore, is in sharp contrast to many recent models that treat a mineral surface undergoing dissolution as a relatively inert substrate to which one can apply the principles of adsorption and simple molecular rates.

Besides revealing the emergence of  $\Delta G$  within a fully kinetic model (atomistic), the kinetic approach was also able to unravel the reasons for both inhibition effects and the appropriateness of product-like phenomenological rate laws. It is clear that future emphasis on clarifying the implications of a crystal-based many-body kinetic approach to our current concepts of how minerals dissolve both in the lab and in nature will be quite fruitful and promise to advance the field of water–rock kinetics in a major way.

**Acknowledgment.** The authors thank R. S. Arvidson, M. S. Beig, T. A. Fewless, M. D. Vinson, and L. Zhang for critical comments and helpful discussions that considerably improved this paper. Reviews by three anonymous referees were especially helpful. The authors gratefully acknowledge support for this study from the Department of Energy (grant nos. DE-FG07-01ER63295, DE-FG02-90ER14153, DE-FG03-02ER63427, USC PO 077944), the National Science Foundation (grant nos. EAR-0125667, EAR-9628238, and EAR-9526794), and the Nanoscale Science and Engineering Initiative of the National Science Foundation under NSF award no. EEC-0118007.

## References and Notes

- (1) Pimpinelli, A.; Villain, J. *The Physics of Crystal Growth*; Cambridge University Press: Cambridge, 1998.
- (2) Lasaga, A. C. *Kinetic Theory in the Earth Sciences*; Princeton University Press: Princeton, NJ, 1998.
- (3) Nielsen, A. E. In *Geochemical Processes at Mineral Surfaces*; Davis, J. A., Hayes, K. F., Eds.; ACS Symposium Series 323; American Chemical Society: Washington, D. C., 1986.
- (4) Lasaga, A. C.; Lüttge, A. *Science* **2001**, *291*, 2400.
- (5) Lasaga, A. C.; Lüttge, A. *Eur. J. Mineral.* **2003**, *15*, 603.
- (6) Ohara, M.; Reid, R. C. *Modeling crystal growth rates from solution*; Prentice-Hall: Englewood Cliffs, NJ, 1973.
- (7) *Rev. Mineral.* **1996**, *34*, 438 pp.
- (8) *Rev. Mineral.* **1995**, *31*, 583 pp.
- (9) Boudart, M. *J. Phys. Chem.* **1976**, *80*, 2869.
- (10) Weeks, J. D.; Gilmer, G. H. *Adv. Chem. Phys.* **1979**, *40*, 157.
- (11) Gilmer, G. H. *J. Cryst. Growth* **1976**, *35*, 15.
- (12) Gilmer, G. H. *J. Cryst. Growth* **1977**, *42*, 3.



- (13) Gilmer, G. H. *Science* **1980**, 208, 355.
- (14) Aagaard, P.; Helgeson, H. *Am. J. Sci.* **1982**, 282, 237.
- (15) Lasaga, A. C. *Am. J. Sci.* **1982**, 282, 1264.
- (16) Lasaga, A. C.; Lüttge, A. *Am. Mineral.* **2004a**, 89, 527.
- (17) Lüttge, A.; Lasaga, A. C. *Chem. Geol.* 2004, submitted for publication.
- (18) Prigogine, I. *Introduction to thermodynamics of irreversible processes*; Interscience: New York, 1967.
- (19) Tang, R.; Nancollas, G. H.; Orme, C. A. *J. Am. Chem. Soc.* **2001**, 123, 5437.
- (20) Tang, R.; Orme, C. A.; Nancollas, G. H. *J. Phys. Chem. B* **2003**, 107, 10653.
- (21) Lasaga, A. C.; Lüttge, A. *Eur. J. Mineral.* **2004b**, 16, 713.
- (22) Bum, A. E.; Stillings, L. L. *Rev. Mineral.* **1995**, 31, 291.
- (23) Lasaga, A. C. *Rev. Mineral.* **1995**, 31, 23.
- (24) Chou, L.; Wollast, R. *Am. J. Sci.* **1985**, 285, 963.
- (25) Gautier, J. M.; Oelkers, E. H.; Schott, J. *Geochim. Cosmochim. Acta* **1994**, 58, 4546.
- (26) Casey, W. H.; Westrich, H. R.; Holdren, G. R. *Am. Mineral.* **1991**, 76, 211.
- (27) Xiao, Y.; Lüttge, A. Unpublished, 2004.
- (28) Blum, A. E.; Lasaga, A. C. *Nature* **1988**, 331, 431.